Geomechanics and Engineering, *Vol. 18, No. 4 (2019) 391-406*
DOI: https://doi.org/10.12989/gae.2019.18.4.391

Bearing capacity of foundation on rock mass depending on footing shape and interface roughness

Ana S. Alencar*[1], Rubén A. Galindo[1a] and Svetlana Melentijevic[2b]

[1]*ETSI Caminos, C. y P., Technical University of Madrid (UPM), C/ Profesor Aranguren s/n, Madrid 28040, Spain*
[2]*Faculty of Geology, Complutense University of Madrid (UCM), C/ José Antonio Nováis nº 2, Madrid 28040, Spain*

(Received March 5, 2019, Revised June 27, 2019, Accepted July 1, 2019)

Abstract. The aim of this paper was to study the influence of the footing shape and the effect of the roughness of the foundation base on the bearing capacity of shallow foundations on rock masses. For this purpose the finite difference method was used to analyze the bearing capacity of various types and states of rock masses under the assumption of Hoek-Brown failure criterion, for both plane strain and axisymmetric model, and considering smooth and rough interface. The results were analyzed based on a sensitivity study of four varying parameters: foundation width, rock material constant (mo), uniaxial compressive strength and geological strength index. Knowing how each parameter influences the bearing capacity depending on the footing shape (circular vs strip footing) and the footing base interface roughness (smooth vs rough), two correlation factors were developed to estimate the percentage increase of the ultimate bearing capacity as a function of the footing shape and the roughness of the footing base interface.

Keywords: circular footing; strip footing; interface; roughness; rock mass; finite difference method

1. Introduction

Among the influencing factors on the ultimate bearing capacity of the shallow foundations on rock mass two issues have not been extensively studied: the influence of the footing shape (Carter and Kulhawy (1988), Clausen (2013), Ramamurthy (2014), Chakraborty and Kumar (2015) and Keshavarz and Kumar (2018)) and the foundation base roughness (no literature about this issue was found in rock mechanics). In soil mechanic, however, the influence of both topics is already recognized, and there are different correction factors published for specific soil type. Regarding the footing shape the studies performed by Meyerhof (1963), De Beer (1970), Brinch Hansen (1970), Anil *et al.* (2017) can be mentioned; while the interface roughness the following authors made significant contributions, Terzaghi, (1943), Meyerhof (1955) and Hjiaj *et al.* (2005), Samanta *et al.* (2018).

Based on the Hoek and Brown failure criterion (1980), Carter and Kulhawy (1988) proposed two formulations to estimate the ultimate bearing capacity for the strip and the circular footing, based on the lower bound solution by adopting the hypothesis of the weightless rock mass.

According to Clausen (2013) there are no systematic results in the literature on the bearing capacity of circular footings resting on a generalized Hoek–Brown failure criterion. Clausen claims that there is no correction factor to estimate how much load a circular footing can support more than a strip footing as a consequence of only its geometry. Therefore, a bearing capacity factor for circular footing was proposed by the same author, that allows the bearing capacity of a circular footing on the rock mass to be estimated by multiplying the uniaxial compressive strength of the intact rock mass (UCS) by this coefficient.

Chakraborty and Kumar (2015) emphasized that there is no literature regarding the influence of the footing shape on the bearing capacity of rock mass. These authors proposed a methodology to determine the bearing capacity of a circular footing over rock mass based on the quasi lower bound limit analysis, in conjunction with the finite element method and the non-linear optimization.

Ramamurthy (2014) suggested that the square or the circular footing resting on the rock mass support 20% more load than a strip footing of the same width. Ramamurthy (2014) approach was to estimate the bearing capacity by the formulation given by Carter and Kulhawy (1988) for strip foundation and increase its results by 20% to obtain the bearing capacity for a square or circular footing.

On the other hand, in soil mechanics the shape coefficient is commonly used. According to Vesic (1973) the engineering approach to evaluate the effect of the foundation shape on the bearing capacity of soil has been mostly semi-empirical, because of the considerable mathematical difficulties to obtain a solution.

Clausen (2013) observed that the use of the equivalent Mohr-Coulomb parameters on the Terzaghi bearing capacity formula can overestimate the bearing capacity of circular surface footings resting on a rock mass by up to 503%.

*Corresponding author, Ph.D. Student
E-mail: at.santos@alumnos.upm.es
[a]Professor
E-mail: rubenangel.galindo@upm.es
[b]Professor
E-mail: svmelent@ucm.es

ISSN: 2005-307X (Print), 2092-6219 (Online)

In this paper, we report the results obtained by the finite difference method employing the commercial code FLAC (2007) that were quantitatively analyzed to define the increase of the bearing capacity due to the shape of the footing depending on the rock mass type. The study of the influence of the geometrical and geotechnical parameters - rock material constant (m_o), footing width (B), uniaxial compressive strength (UCS) and geological strength index (GSI)- were done to obtain a shape correction factor (C_F) to add as additional bearing capacity due to the circular shape. The diameter of the circular foundation was considered equal to the width of the strip foundation. Furthermore, an analysis of the horizontal and vertical displacement of the rock mass observed below the foundation was also done. Therefore, the bearing capacity can be estimated by the analytical formulation for the strip footing such as that proposed by Serrano *et al.* (2000) or Carter and Kulhawy (1988) and the result can be fitted for the circular footing applying the proposed shape correction factor (C_F).

The second topic of this paper is the influence of the footing base interface roughness on the bearing capacity of the rock mass for which we could not find any published papers in rock mechanics. Studies on roughness in rock mechanics usually focus on the joints of rock mass (Barton (1973), Barton and Choubey (1977), Tse and Cruden (1979), Du *et al.* (2015), Tikou (2016)), the shear resistance to evaluate the sliding stability of dam founded on rock (Lo *et al.* (1990, 1991), Ghos (2010), Krounis *et al.* (2016), Mouzannar *et al.* (2017)) or papers related to the shaft resistance of the pile embedded in rock (Pells *et al.* (1980), Rowe and Armitage (1984), Seidel and Collingwood (2001), Nam and Vipulandan (2008), Jeong et al (2010), Melentijevic and Olalla (2014), Gutiérrez-Ch *et al.* (2018)).

The analytical solution proposed by Serrano *et al.* (2000) to estimate the bearing capacity, does not take into account the roughness of the foundation base, because the formulation does not consider the displacement hypothesis. The Serrano & Olalla solution for the Hoek-Brown failure criterion (1997) uses the characteristic line method (Sokolovskii, 1965). In the analytical formulation, a uniform distribution of the vertical stress on the ground surface is assumed but the presence of the shear stress on the support level is not considered.

The bearing capacity charts for strip footings (Merifield (2006)) and circular footings (Clausen (2013)), based on the GSI system, are given for a rough interface of the foundation base without elaborating the associated failure mechanism.

Meyerhof (1955) showed in soil mechanics that theoretically in cases under the assumption of the weightless material the bearing capacity is independent from the interface roughness. The interface roughness is associated with the self-weight of the material because the friction of the surface changes the shape and the size of the wedge (Meyerhof (1955), Hjiaj *et al.* (2005)). Therefore, depending on the interface type, the failure affects a different amount of the ground material. Hjiaj *et al.* (2005) observed that in cases of cohesionless material the size of the wedge for a smooth footing is smaller than that for an equivalent rough footing. According to Jahanandish *et al.* (2012), for the frictional soils with relatively high internal friction angles, the bearing capacity of the foundation with a rough base is approximately two to three times higher than those for the foundation with the smooth base with the stress level taken into consideration. It is emphasized that the influence of the interface roughness on the bearing capacity, in soil material, depends on the embedment depth (Meyerhof (1955), Benmebarek *et al.* (2017)). With the increase of the embedment depth, the influence of the base interface decreases, and the lateral interface becomes more important. Considering that, under the hypothesis of the footing supported on the ground surface, the maximum influence of the base interface can be obtained.

In cases of rock mass, the influence of the base roughness of the footing on the bearing capacity is of great interest, because the rock mass resistance can be equal to or higher than the concrete resistance. However, the analytical solution (Serrano *et al.* (2000)) cannot take into account this hypothesis (base roughness) because it does not include the displacement of the footing nor the footing stiffness effect in its theoretical formulation.

In this paper we studied the influence of the base interface of the footing by applying the numerical analysis, taking into consideration the footing directly supported at the surface level, without embedment. The variation of the bearing capacity was analyzed according to the interface roughness, based on geometrical and geotechnical parameters (m_o, B, UCS and GSI). A roughness correlation factor R_F is proposed, that can be used to estimate the percentage of the variation of the bearing capacity due to the interface roughness. Finally, the size and the shape of the wedge below the foundation was also analyzed by considering the outputs of the displacements (horizontal and vertical) developed below the foundation.

2. Numerical analysis

A total of 192 cases of rock masses were analyzed, resulting from the combination of four influential parameters in the ultimate bearing capacity. The values of these parameters are given in Table 1 that covers a wide variety of types and states of rock masses.

Numerical calculations were developed by the finite difference method employing 2D models and applying the plane-strain condition to represent a strip footing and the axisymmetry condition to simulate a circular footing. A cylindrical coordinate system was used in the axisymmetric model that can represent objects with axial symmetry, for example a circular footing. A symmetrical model is used in the case of the plane-strain condition where only half of the strip footing is represented (see Fig. 1). The axisymmetric grid is viewed as a unit-radian sector (FLAC, 2007). The boundaries of both models are located at a distance that does not interfere with the result.

From the basic cases, five different calculation hypotheses were implemented (Table 2), resulting in a total of 960 cases. The rock mass was considered both under the assumption of the weightless rock mass and taking into account the self-weight of the rock mass with the unit weight of 26 kN/m^3. In all simulations the associative flow rule was adopted and the Modified Hoek-Brown

Table 1 Summary of the adopted parameters

m_o	B (m)	UCS (MPa)	GSI
5 (Claystone)	4.5	5	10
12 (Gypsum)	11	10	50
20 (Sandstone)	16.5	50	85
32 (Granite)	22	100	

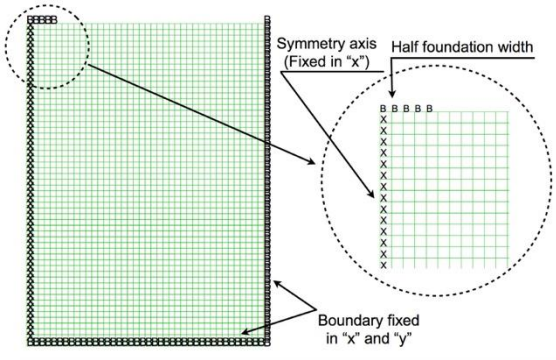

Fig. 1 2D model used

Table 2 Hypothesis adopted for numerical analysis

Models type	Weight	Interface	Hypothesis adopted in Section
Axisymmetric	Weightless	Rough	3
Plane-strain	Weightless	Rough	3
Plane-strain	Self-weight	Rough	4
Plane-strain	Self-weight	Smooth	4
Plane-strain	Weightless	Smooth	4

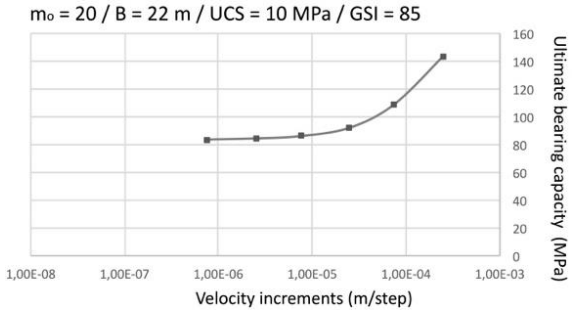

Fig. 2 The ultimate bearing capacity-velocity increments diagram of the central node of the foundation

constitutive model, available in FLAC v.7, was used.

It is assumed that numerically the ultimate bearing capacity is reached when the continuous medium not support more load, because an internal failure mechanism had been formed. In FLAC the load is applied through velocity increments, and the ultimate bearing capacity is determined from the relation between stresses and displacements of one of the nodes; in this case the central node of the foundation was considered.

A convergence study was also performed that consisted in the analysis of values of the ultimate bearing capacity that was obtained under different increments of velocity used (Fig. 2).

Fig. 2 shows the dependence of the result of the ultimate bearing capacity in relation to the velocity increments applied on the nodes and how with the decrease in the value of velocity increments the result converges towards the final value by the upper limit in the theoretical method. For each case with different combination of geometrical and geotechnical parameters (Table 1) a convergence study was carried out with different values of velocity increments.

It is important to note that in the numerical calculations the model was usually simplified by adopting a footing as a load (velocity increments) applied directly on the ground surface. Thus, it was not necessary to define strength parameters for the footing, neither for the interface between the ground and the structure. To simulate a perfectly smooth or rough interface, the nodes where the load is applied are loose or fixed, allowing or not the displacement.

In the cases studied, the vertical load was applied by velocity increments: if the nodes where the load was applied were fixed in two perpendicular directions ("x" and "y") the interface was perfectly rough. When the movement in the horizontal direction ("x") was not restricted, a perfectly smooth interface was simulated, because there was no resistance to the horizontal movement.

We must emphasis that analytically the bearing capacity only depends on the interface roughness in cases where the self-weight of the material is considered. However, numerically it was observed in our cases that under the hypothesis of the weightless rock mass the bearing capacity depends on the interface type as well. This is due to the fact that analytically the stress state in failure is studied, while numerically a stress path is carried out until the failure is reached.

3. The influence of the footing shape

As generally known, a circular footing supports more load than the strip footing of the same width. This is because the resistance mechanism of the circular footing is developed in 3D. Under the plastic hypothesis, a behavior of a strip footing can be simulated by several rectangles placed next to each other. The result is an overlapping of the bulbs of pressure reaching greater depths, and these pressure bulb depth differences can be expected at the failure (elastic behaviour).

Regarding the difference between the circular and the square footing, the circular footing supports more load, because there are no vertices; weakness points that reduce the bearing capacity. It is considered that the bearing capacity of the strip and the circular footing are the upper and the lower limits as function of the shape.

In this section were studied: the influence of the footing shape on the bearing capacity under the assumption of the weightless rock mass; the associative flow law; the rough interface.

3.1 Results of the analysis

As anticipated, the results of the bearing capacity obtained with the axisymmetric model (P_{hCF}) for a circular footing, are greater than the calculated footing under plane strain conditions (P_{hSF}) that simulate a strip footing. So, the

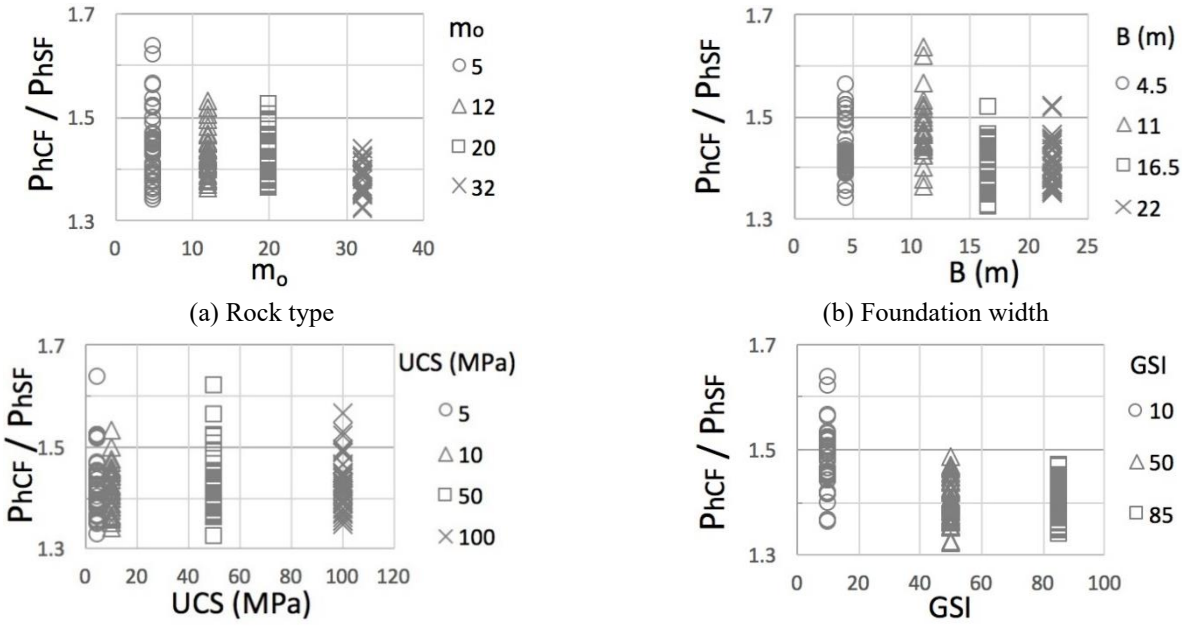

(a) Rock type (b) Foundation width

(c) UCS (d) GSI

Fig. 3 Correlation between P_{hCF} and P_{hSF}, depending on m_o, B, UCS and GSI

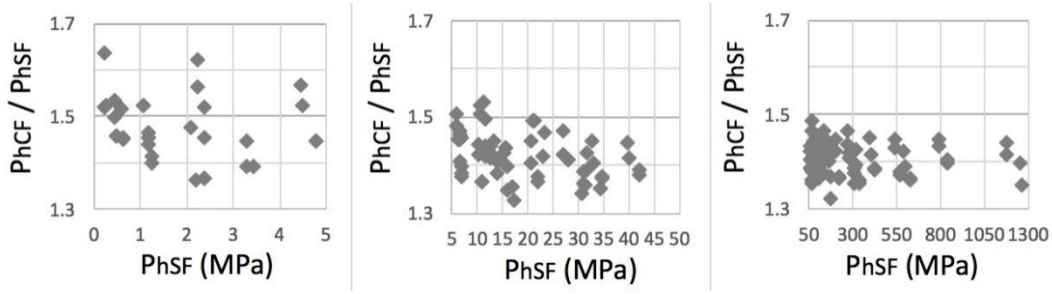

Fig. 4 Correlation between P_{hCF} and P_{hSF} depending on P_{hSF}

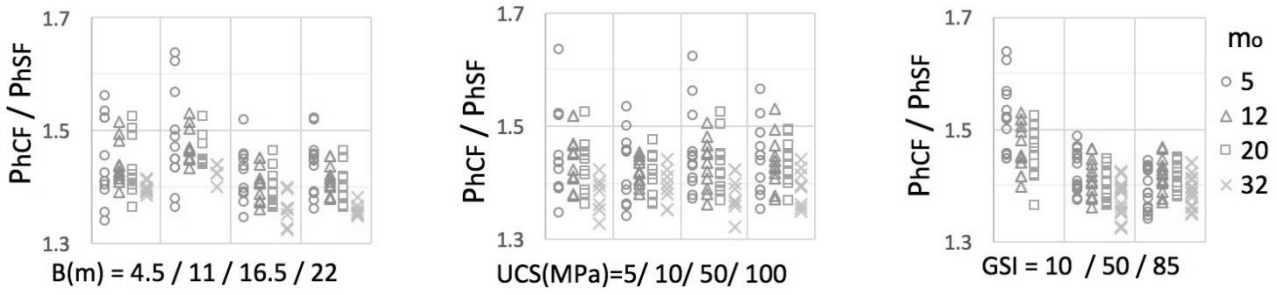

(a) Foundation width (b) UCS (c) GSI

Fig. 5 Correlation between P_{hCF} and P_{hSF} depending on m_o

correlation can be expressed as in Eq. (1), taking into account that everything was divided by the lowest value of the bearing capacity (P_{hSF}), thus making the equation dimensionless. With factor C_F we could estimate the percentage of the bearing capacity that the circular footing supports more than the strip footing of the same width; assuming the diameter of the circular foundation was equal to the width of the strip foundation.

$$\frac{P_{h_{CF.}}}{P_{h_{SF}}} = 1 + \frac{\Delta P_h}{P_{h_{SF}}} = 1 + C_F \quad (1)$$

Fig. 3 shows the correlation between P_{hCF} and P_{hSF} as a function of four variable parameters summarized in Table 1. In each graphic parameter is highlighted (m_o in Fig. 3(a), B Fig. 3(b), UCS Fig. 3(c) and GSI Fig. 3(d)). If the dispersion ranges of each parameter changes in function of the value (represented in the abscissa axis), it means that the parameter influences the relation between P_{hCF} and P_{hSF}.

Due to numerical instability problems of the model, it was not possible to obtain a numerical result for a combination of m_o = 32 and GSI = 10 with different values of UCS and B, under the hypothesis of plane-strain,

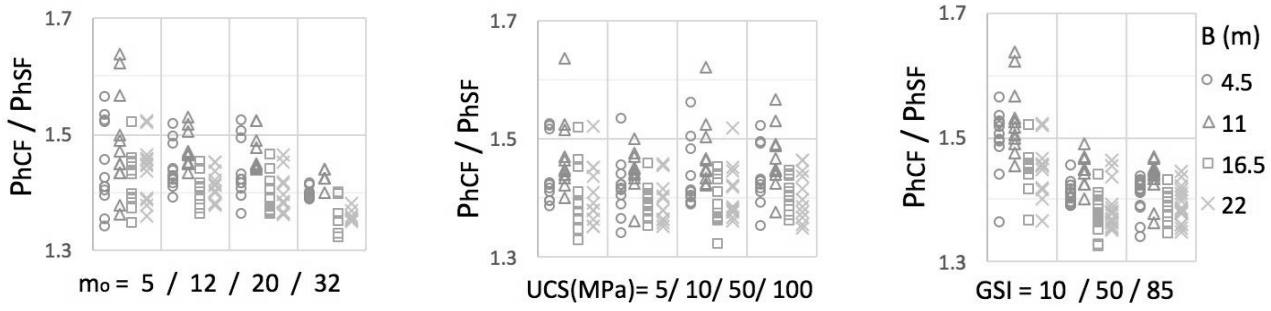

(a) Rock type (b) UCS (c) GSI

Fig. 6 Correlation between P_{hCF} and P_{hSF} depending on B

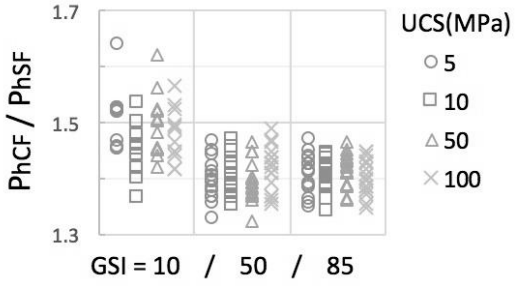

Fig. 7 Correlation between P_{hCF} and P_{hSF} depending UCS and GSI

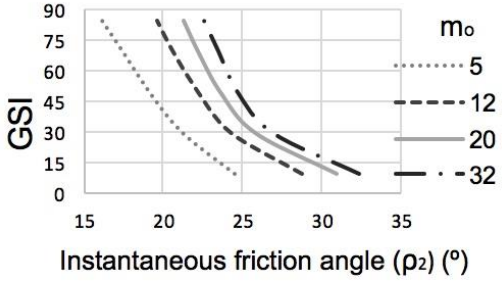

Fig. 8 Instantaneous friction angle as function of GSI

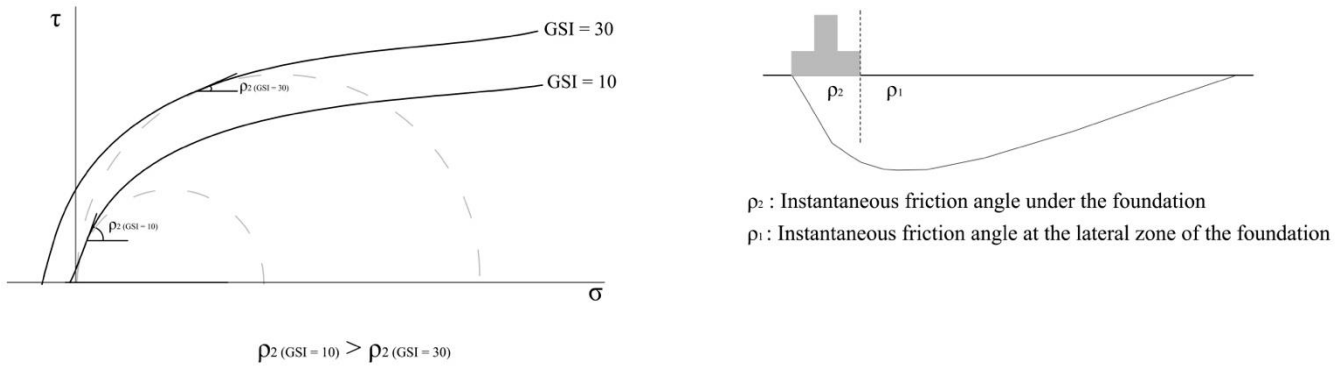

Fig. 9 Instantaneous friction angle schedule adapted from Serrano *et al.* (2000)

weightless rock mass and the associative flow law. Therefore, the variations in the results presented in the figures do not cover all the cases that were analyzed.

In Fig. 3(a) the results for m_o = 32 are not representing the greater dispersion as expected due to instability problems of the numerical model. Fig. 3(d) shows the dispersion of the results of P_{hCF} and P_{hSF} depending on the GSI and it can be observed that for lower GSI the variation between P_{hCF} and P_{hSF} is the greatest. With GSI=10 the range of dispersion varies from 35 to 65%, while for medium and higher values of GSI, the range is between 35 and 50%. From Fig. 3 the most influential parameter on the bearing capacity was GSI.

On the other hand, Fig. 3(b) and 3(c) do not clearly demonstrate the influence of parameters B and UCS in correlation between P_{hCF} and P_{hSF}, because in both parts the

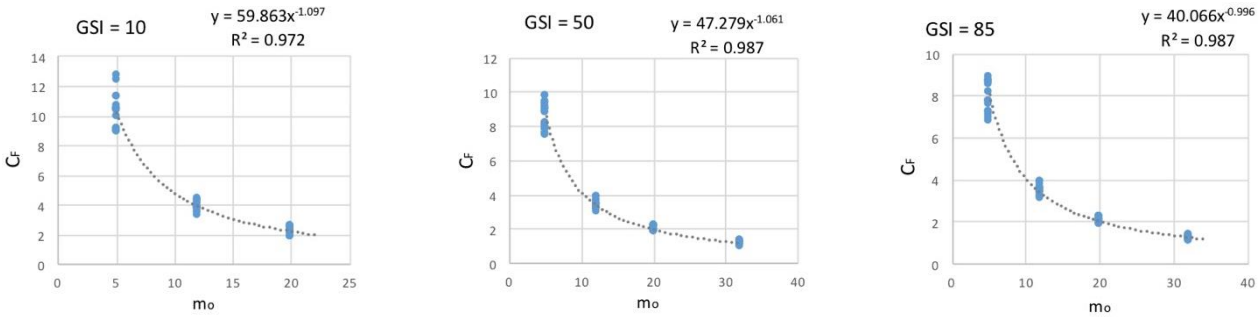

(a) GSI = 10 (b) GSI = 50 (c) GSI =85

Fig. 10 C_F in function of m_o for different values of GSI

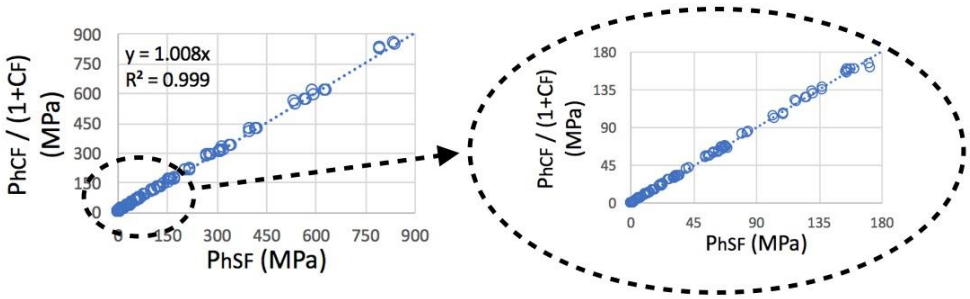

Fig. 11 Correlation of bearing capacity obtained with the Eq. (2)

dispersion range did not show a noticeable trend. In fact, a wide range of the values were observed between P_{hCF} / P_{hSF} independent of the value of parameters B and UCS. Indeed, Fig. 4 was developed to study a global interpretation of the influence of all parameters on the bearing capacity by means of the correlation between P_{hCF}/P_{hSF} and P_{hSF}. From Fig. 4 it can be concluded that bearing capacities greater than 12 MPa were conditioned by the shape of the foundation between 35 to 50%. For bearing capacities lower than approximately 12 MPa, there was a greater dispersion (P_{hCF}/P_{hSF}) ranging from 35 to 65%.

Fig. 5 shows the same results as given in Fig. 3(a), subdivided by the rock type (m_o), to analyze the combined influence of the mo with other parameters (B, UCS and GSI).

From Fig. 5(a)-(b) a general trend can be observed regarding the decrease of the P_{hCF}/P_{hSF} with the increase of the mo. However, in the absence of the most dispersed results for m_o = 32 (with GSI = 10), but this observation is not completely accurate.

In Fig. 5(c) the missing results would form a separate column, and it can be observed that with a lower GSI the dispersion range is more dependent on the values of the mo. However, for medium and higher values of GSI, the value of mo slightly changes the dispersion of the results that leads to the conclusion that the influence of the mo depends on the overall geotechnical quality of the rock mass (GSI).

Fig. 3(b), Fig. 5(a) and Fig. 6 show that the influence of the footing width is not constant for B=11m, which is an intermediate value, when the maximum variation is observed.

In the same way, the influence of the UCS cannot be observed in Fig. 3(c), Fig. 5(b) and Fig. 6(b) considering that independently of the value of the UCS, the dispersion

Table 3 Equations of C_F depending on m_o, for different values of GSI

GSI	Equations
10	$C_F = 59.863 \cdot m_o^{1.097}$
50	$C_F = 47.279 \cdot m_o^{1.061}$
85	$C_F = 40.066 \cdot m_o^{0.996}$

of the results of P_{hCF} and P_{hSF} were very similar.

Regarding Fig. 7 a slight increase in the dispersion range of results obtained with low value of GSI can be observed. Thus the UCS influences equally the bearing capacity estimate in the plane-strain and in the axisymmetric model, with which this parameter does not condition the correlation of the results.

Finally, from our analysis the GSI was the most influential parameter in the relationship between P_{hCF} and P_{hSF}. This observation can be justified because the instantaneous friction angle is heavily dependent on the GSI, and in soil mechanics the friction angle is one of the parameters used to estimate the shape factor (De Beer (1970)).

Fig. 8 shows how the instantaneous friction angle under foundation (ρ_2) (Serrano *et al.* (2000)) varies depending on the GSI value. From Fig. 9 it can be deduced that for lower value of GSI the ρ_2 is greater, because the failure occurs when associated with low stress status, where the instantaneous friction angle is higher.

It is important to emphasize that low quality granular soils present a low internal friction angle, so the influence of the shape factor is small. However, poor quality rock mass (related to low GSI values) shows higher instantaneous friction angles, so in cases of rock mass, the

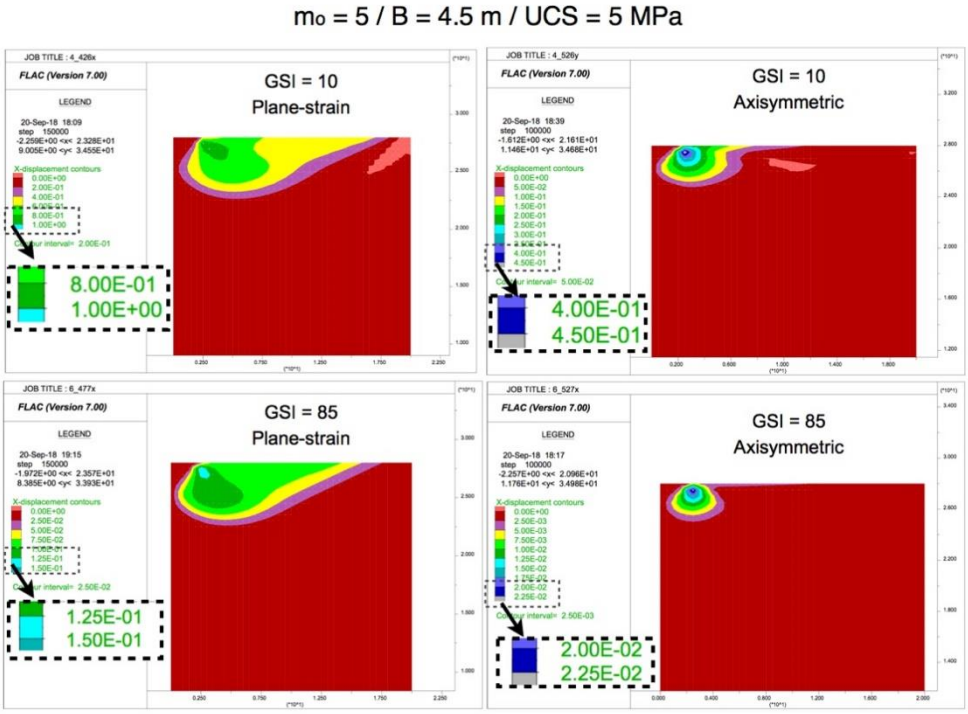

Fig. 12 The variation of horizontal displacements under the foundation as a function of GSI

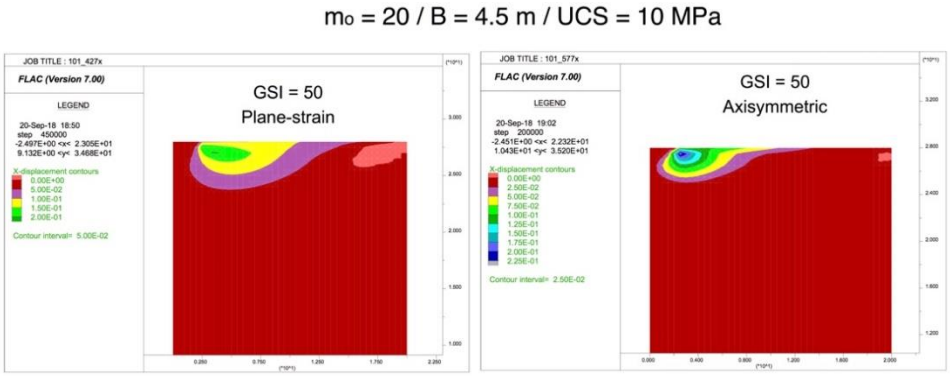

Fig. 13 The variation of horizontal displacements under the foundation

influence of the footing shape on the bearing capacity is more significant for high weathered rock mass. For example, it can be observed in Fig. 7 that the greater dispersion range are associated with GSI = 10, between 35 to 65%, while for the medium and high values of GSI are lower than 50%.

3.2 Coefficient C_F

Knowing that the most influential parameters are GSI and mo, the correlation of the results for each value of the GSI was analyzed according to rock type (m_o) (Fig. 10) resulting in formulating three equations (Table 3).

Therefore, since the equations in Table 3 have the same structure, a single equation based on GSI can be formulated (Eq. (2)), by which we could estimate the percentage of the bearing capacity that the circular footing support more than the strip footing of the same width; considering that the diameter is equal to the width.

$$C_F = \left(\frac{250 - GSI}{4}\right) \cdot m_o^{\frac{1.2 \cdot (GSI-100)}{1000}} \quad (2)$$

In the graph in Fig. 11 it can be seen that the percentage change calculated by Eq. (2) was actually observed in 192 of the cases studied, with a variation between the results that did not exceed 1%. So this coefficient (C_F) can be used in conjunction with the usual formulation for the bearing capacity of the strip footing such as those proposed by Serrano *et al.* (2000) or Carter and Kulhawy (1988), to semi-analytically estimate the bearing capacity considering a circular footing.

3.3 Displacement analysis

In the numerical calculation to estimate the bearing capacity a stress path is formed until failure is reached, taking into account the whole wedge of the ground below the foundation. Therefore, the graphic outputs of the

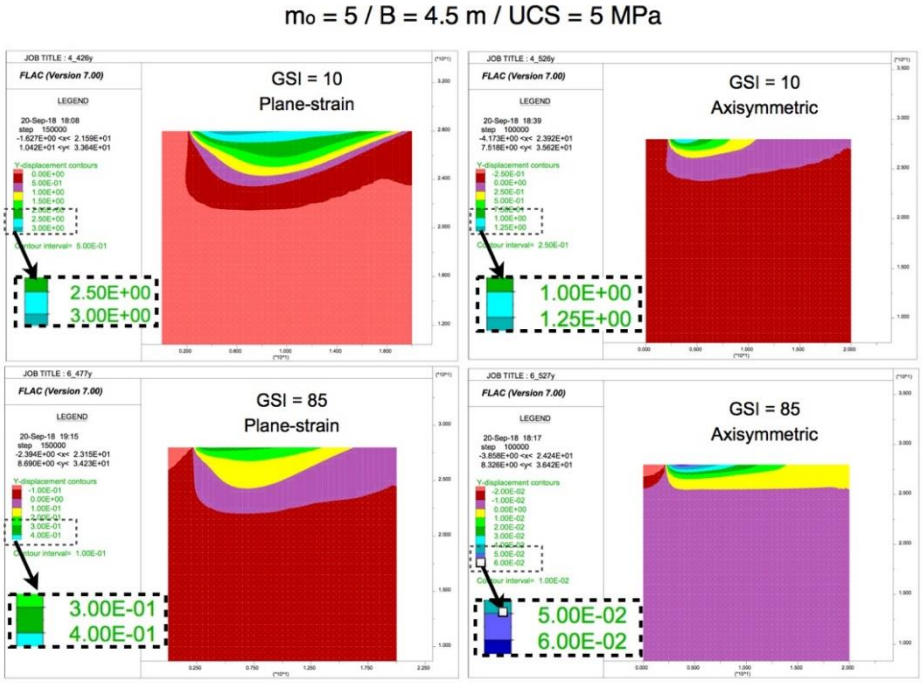

Fig. 14 The variation of vertical displacements under the foundation as a function of GSI

displacements (horizontal and vertical) developed below the foundation were used to understand how the failure mechanism affects the results.

In both models, the horizontal displacement decreases when the GSI increases (Fig. 12). In the axisymmetric model, in cases of low mo, the horizontal displacement was concentrated close to the footing edge presenting different shapes of the wedge in function of the increase of GSI. However, for high values of mo the shape of horizontal displacements was similar to a wedge, so the lateral boundary of the foundation was more affected in these cases (Fig. 13).

Regarding the vertical displacement, it was observed in both models that for high values of m_o and GSI the displacement limits (wedge) was best defined in (Fig. 14). Confirming the theory, the vertical displacements were deeper in the plane-strain model compared to the axisymmetric model (Fig. 13).

3.4 Example of the application and comparison of the results

To semi-analytically estimate the bearing capacity of a circular footing, the bearing capacity was first calculated for a strip footing following the Serrano *et al.* (2000) method and the result was then increased by applying Eq. (2).

$$P_h = (1 + C_F) \cdot P_{hs\&O} \quad (3)$$

The results obtained by eq. (3) are presented in Table 4 in the column "semi-analytical".

To compare the results of the bearing capacity of rock mass obtained by different methods can be done through the bearing capacity factor (N_σ). For circular footing the abbreviation adopted for the bearing capacity factor was $N_{\sigma C}$ (Clausen (2013)).

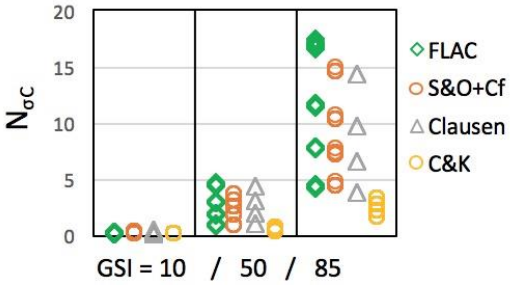

Fig. 15 $N_{\sigma C}$ as function of GSI

Table 4 Comparison of $N_{\sigma C}$ values

Parameters				$N_{\sigma C}$			
m_o	B	UCS (MPa)	GSI	FDM	Semi-analytical (C_F)	Clausen (2013)	Carter and Kulhawy (1988)
5	11	100	10	0.07	0.07	0.07	0.04
5	11	100	50	0.97	0.94	1.05	0.3
5	11	100	85	4.23	4.33	3.8	1.64
12	4.5	50	10	0.17	0.14	0.18	0.06
12	4.5	50	50	1.85	1.71	1.95	0.42
12	4.5	50	85	7.74	7.24	6.6	2.23
32	16.5	5	10	0.6	0.38	0.52	0.1
32	16.5	5	50	4.54	3.11	4.45	0.64
32	16.5	5	85	17.16	14.62	14.3	3.32

This factor multiplied by the UCS enabled us to determine the bearing capacity, as in Eq. (4).

$$P_h = N_{\sigma C} \cdot UCS \quad (4)$$

Carter and Kulhawy (1988) and Clausen (2013) proposed a formulation to estimate the bearing capacity

factor $N_{\sigma C}$ in function of the parameters of the Hoek-Brown failure criterion (m_o, GSI and UCS). Serrano *et al.* (2000) proposed a bearing capacity factor Nσ for strip footing that by applying the factor C_F by eq. (2) becomes a $N_{\sigma C}$. The results of the bearing capacity obtained numerically by FDM can also be expressed as a function of $N_{\sigma C}$. The $N_{\sigma C}$ values obtained by these four methods are presented in Table 4 and in Fig. 15 for different case studies, considering the hypothesis of the weightless rock mass. There is a big difference between the value of $N_{\sigma C}$ estimated by the formulation proposed by Carter and Kulhawy (1988) and other results (the results can exceed 500%), that present very similar values within the same order of magnitude. According to Carter and Kulhawy (1988) the proposed equation estimates the lower-bound bearing capacity, so it is assumed that the bearing capacity can be higher.

From Fig. 15 it can be concluded that the dispersion range of results increase was associated with the increment of the GSI and that this parameter defines the range of the bearing capacity value.

Comparing $N_{\sigma C}$ calculated by FDM with those estimated by the Clausen (2013) method, we observe the largest variation between the results occurs for higher GSI values (GSI = 85), with the FDM results in the range of 10% to 17% higher than those recommended by Clausen (2013).

The semi-analytical results compared with those obtained by FDM, the semi-analytical values were lower than estimated numerical values. Regarding the influence of the geotechnical parameters the difference between the results increase for high values of mo and low values of GSI. For example, in cases where GSI=10 and m_o=32 the variation between the results can exceed 45%. However, it must be emphasized that the semi-analytical result was lower than the estimated numerical value, so the estimated value is on the conservative side.

3.5 Comparison of the semi-analytical results with the bearing capacity obtained in field tests

Apart from the study of the influence of the footing shape on the bearing capacity for hypothetical rock masses, eighteen real cases were also analyzed including those found in the bibliography. It must be pointed out that in the field tests some specific factors can affect the bearing capacity; such as the scale effect, the developed flow law, the contribution of the self-weight of material, amongst other factors. In the analytical solution considered in this study (Serrano et al, 2000), the adopted hypothesis were the associative flow law, plane strain conditions and the weightless material, while the size of the foundation was not analyzed.

Therefore, it was expected that the results obtained by both the semi-analytical method, i.e., Serrano *et al.* (2000) with factor C_F defined by eq. (2), and the results from the field tests published by different authors, would be similar. However, considering that some hypotheses are different, the results vary as was expected.

Tajeri *et al.* (2015) collected published experimental data of the bearing capacity in shallow foundations by different authors, among them: Maleki and Hollberg (1995), Nitta *et al.* (1995), Pellegrino (1974), Pells and Turner (1979, 1980), Spanovich and Garvin (1979), Williams (1980).

Table 5 Bearing capacity estimated for the different case studies summarized in Tajeri (2015)

Reference	GSI	UCS (MPa)	m_o	C_F (%)	$P_{h(field\ test)}$ (MPa)	$P_{h(S\&O)} + C_F$ (MPa)
Maleki and Hollberg (1995)	62	13.8	7	43	20	26.89
Nitta *et al.* (1995)	80	1.07	32	39	18	12.81
Pellegrino (1974)	70	4.72	13	41	10.53	19.49
	72	4.03	13	41	10	18.00
	70	4.03	13	41	11.16	16.64
	75	3.35	13	41	12	16.90
	65	2	17	41	5.92	8.14
Pells and Turner (1979 & 1980)	65	14	17	41	75.6	57.00
	65	11.61	17	41	72.8	47.27
	80	0.3	17	40	4.5	2.22
	80	0.3	17	40	3.75	2.22
Spanovich and Garvin (1979)	60	1.45	6	44	4.44	2.35
	70	1.45	6	42	6.62	3.64
	50	1.45	6	45	3.47	1.54
Williams (1980)	81	0.54	6	41	4.51	2.16
	81	0.57	6	41	4.98	2.29
	90	0.6	6	39	7.2	3.55
	100	0.44	6	38	10.57	4.04

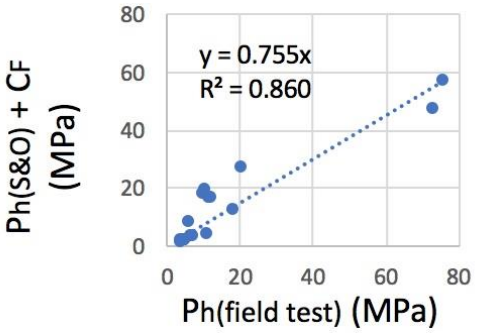

Fig. 16 Correlation of the P_h obtained by semi-analytical way and field tests for data summarized in Table 5

Table 5 shows the geotechnical parameters of those cases where the ultimate bearing capacity was obtained by experimental study, the results from field tests of the ultimate bearing capacity and the result estimated by applying the method proposed by Serrano *et al.* (2000) combined with the shape factor (C_F).

It can be observed in Table 5 that in all cases C_F is in the order of 40%, that corresponds to the range of values of the GSI medium or high. Fig. 16 shows that the correlation between the results is acceptable, considering that many aspects influence the bearing capacity. It must be emphasized that for low values of the bearing capacity the adjustment between the results is better. In addition, according to the results shown in Fig. 16 that for the high values of bearing capacity the results obtained from the

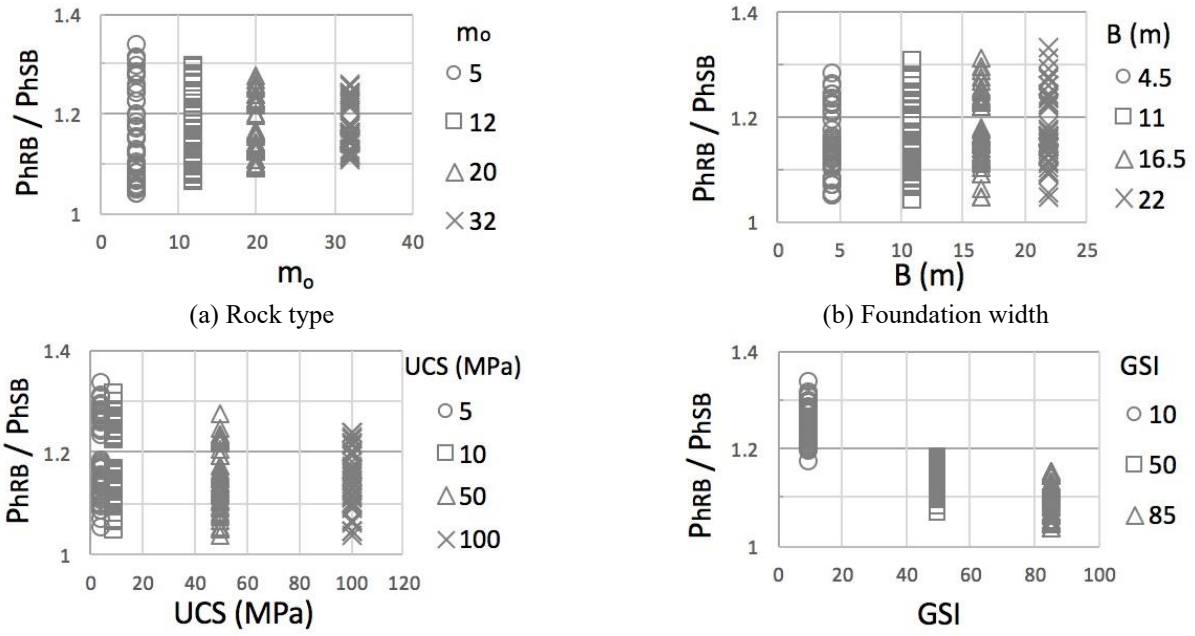

(a) Rock type (b) Foundation width

(c) UCS (d) GSI

Fig. 17 Correlation between P_{hRB} and P_{hRB} depending on m_o, B, UCS and GSI

field test are higher than those estimated by the semi-analytical method.

4. The influence of the base roughness of the footing

The numerical results obtained from the case studies described in Table 1 under the assumption of plane strain condition, associative flow law, self-weight rock mass, and two interface types: (A) rough base (P_{hRB}) and (B) smooth base (P_{hSB}) were analyzed to establish the influence of the interface roughness on the bearing capacity of the rock mass and develop the formulation of the correlation factor R_F; we could visually estimate this variation.

As expected, the values of the bearing capacity calculated considering the rough interface (P_{hRB}) were greater than those estimated for the smooth interface (P_{hSB}). To make the equation dimensionless, it was divided by the lower value of the ultimate bearing capacity (P_{hSB}), resulting in the following equation

$$\frac{P_{h_{RB}}}{P_{h_{SB}}} = 1 + \frac{\Delta P_h}{P_{h_{SB}}} = 1 + R_F \quad (5)$$

The R_F factor represents the percentage of bearing capacity that a footing with a rough interface can support more than a footing with smooth interface of the same width. This coefficient was developed based on the analysis of the influence of the geometrical and geotechnical parameters (m_o, B, UCS and GSI) on the correlation between the P_{hRB} and P_{hSB}. The bearing capacity was calculated by applying the finite difference method; the hypothesis adopted in the numerical model are given in section 2.

Fig. 17 shows the correlation between P_{hRB} and P_{hSB} as a function of four variable parameters summarized in Table 1. The reader is reminded that in Fig. 3 each graphic image highlights a specific parameter (m_o in Fig. 3(a), B Fig. 3(b), UCS Fig. 3(c) and GSI Fig. 3(d)). If the dispersion range for each parameter changed as a function of the value (represented in the abscissa axis) this meant that the parameter influenced the relation between P_{hCF} and P_{hSF}. From Fig. 17 it can be postulated that the two main parameters that had most impact on the relation between P_{hRB} and P_{hSB} were GSI and mo. This is because in the relation between B and UCS, the dispersion range did not shown a noticeable trend, in fact, a wide range of values were observed between P_{hRB} / P_{hSB} independent of the value of parameters B and UCS.

Fig. 17(a) shows that the dispersion range of the results decreases with the increase of mo, e.g., for m_o = 5 the values obtained with rough interface were 3 to 33% higher thanthose calculated for a smooth interface. While, for m_o = 32, the dispersion range varies between 11 to 28%.

Regarding the footing width, Fig. 17(b) shows a slight increase (less than 5 %) in the dispersion of the values of bearing capacity obtained with increasing B. For example, comparing the maximum dispersion for B = 4.5 m is 29%, while for B = 22 m is 33%. Therefore, it can be concluded that the value of B does not exert big influence on the correlation between P_{hSB} and P_{hRB}.

In Fig. 17(d) a decrease in the dispersion range was observed with an increase of GSI. The bearing capacity of the poor quality rock mass (GSI = 10) varies from 20 to 33% depending on the interface type. However, for the average and very good rock mass quality the dispersion range was between 4 and 19%.

Fig. 17(c) shows than the minimum value of correlation was independent of the UCS, as it was close to 3% for all UCS values, while the maximum variation decreased withthe increase of the UCS. In cases of low UCS, such as 5 MPa, the variation between P_{hSB} and P_{hRB} can be up to 35%, while for UCS = 100 MPa the maximum variation was

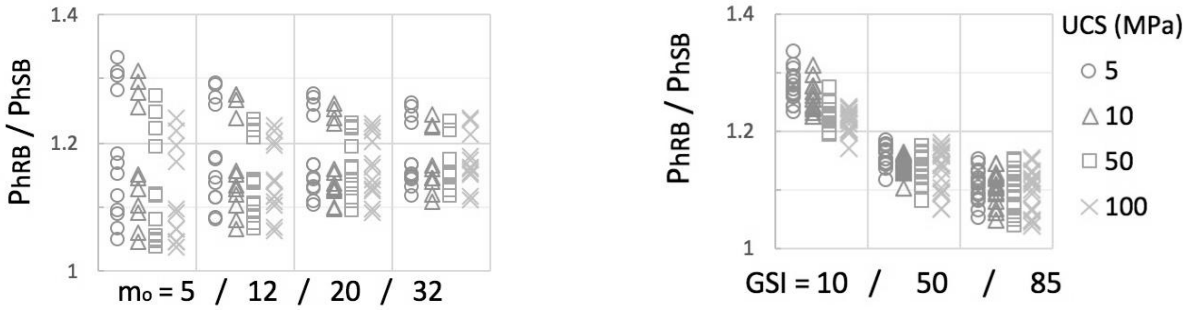

(a) Rock type (b) GSI

Fig. 18 Correlation between P_{hRB} and P_{hSB} depending on UCS, m_o and GSI

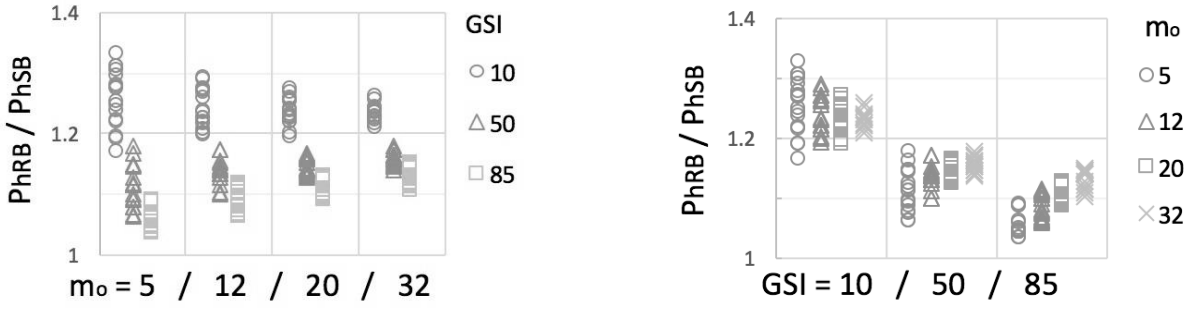

(a) Rock type (b) GSI

Fig. 19 Correlation between P_{hRB} and P_{hSB} depending on m_o and GSI

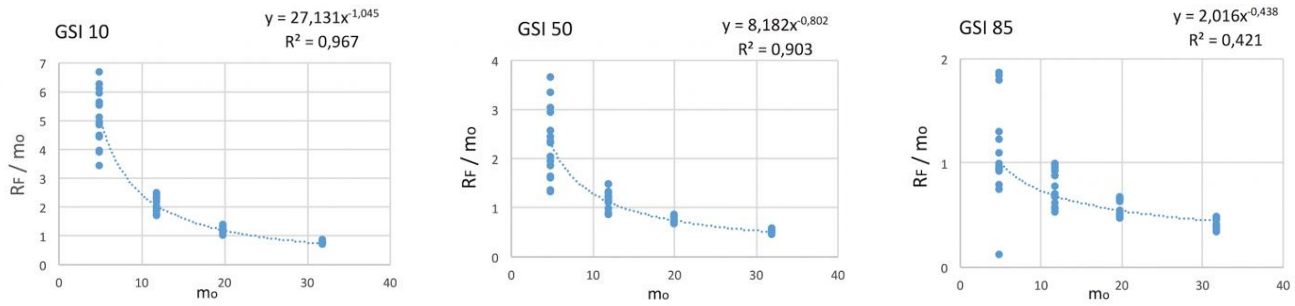

(a) GSI = 10 (b) GSI = 50 (c) GSI =85

Fig. 20 R_F in function of m_o for different values of GSI

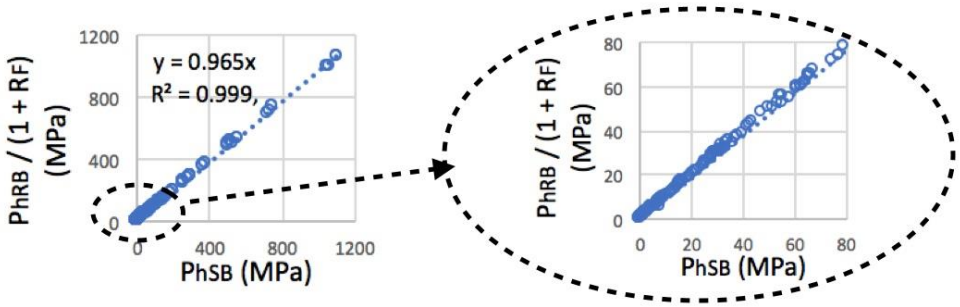

Fig. 21 Correlation of bearing capacity obtained with the Eq. (6)

Table 6 Equations of R_F depending on m_o, for different values of GSI

GSI	Equations
10	$R_F = 27.131 \cdot m_o^{-1.045}$
50	$R_F = 8.182 \cdot m_o^{0.198}$
85	$R_F = 2.016 \cdot m_o^{0.562}$

close to 25%.

The correlation between P_{hRB} and P_{hSB}, depending on UCS, mo and GSI, are given in Fig. 18, where the minimum values of the increment in the bearing capacity was determined by the mo. Concluding that the minimum values of increment is the same for all values of UCS, which were

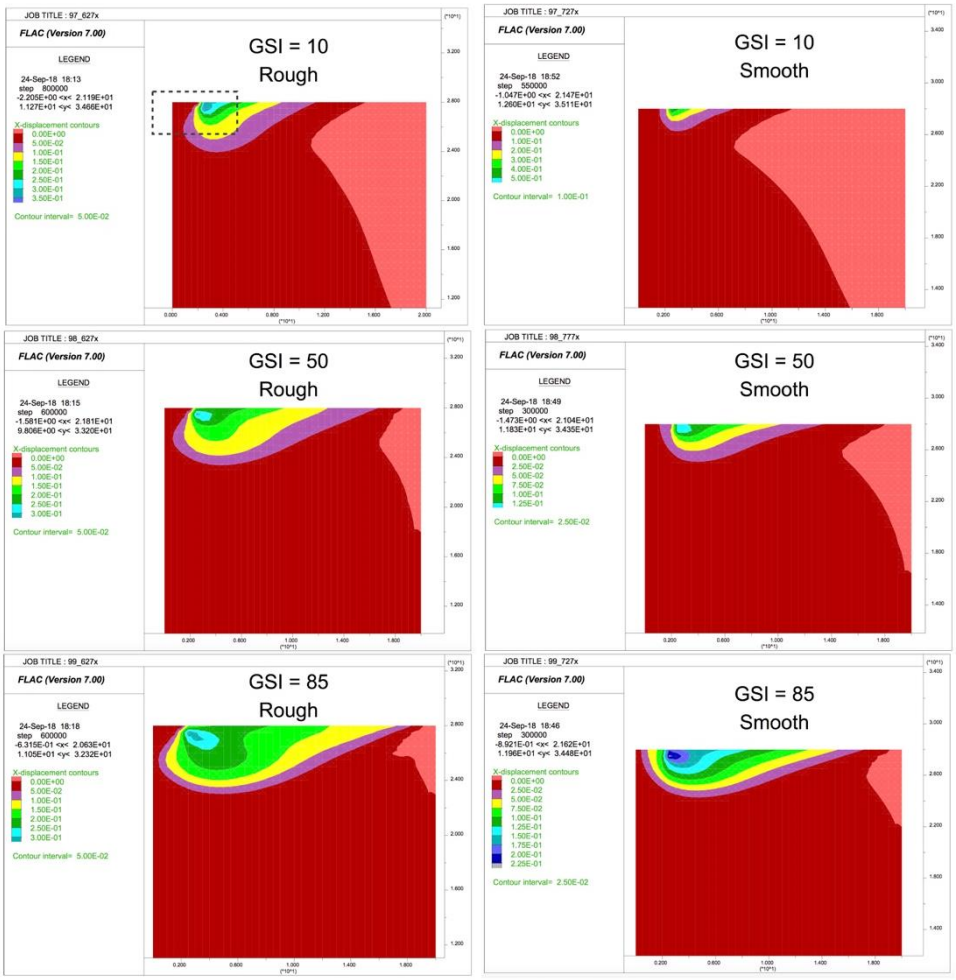

m_o = 20 / B = 4.5 m / UCS = 5 MPa

Fig. 22 The variation of the horizontal displacements under the foundation as a function of GSI

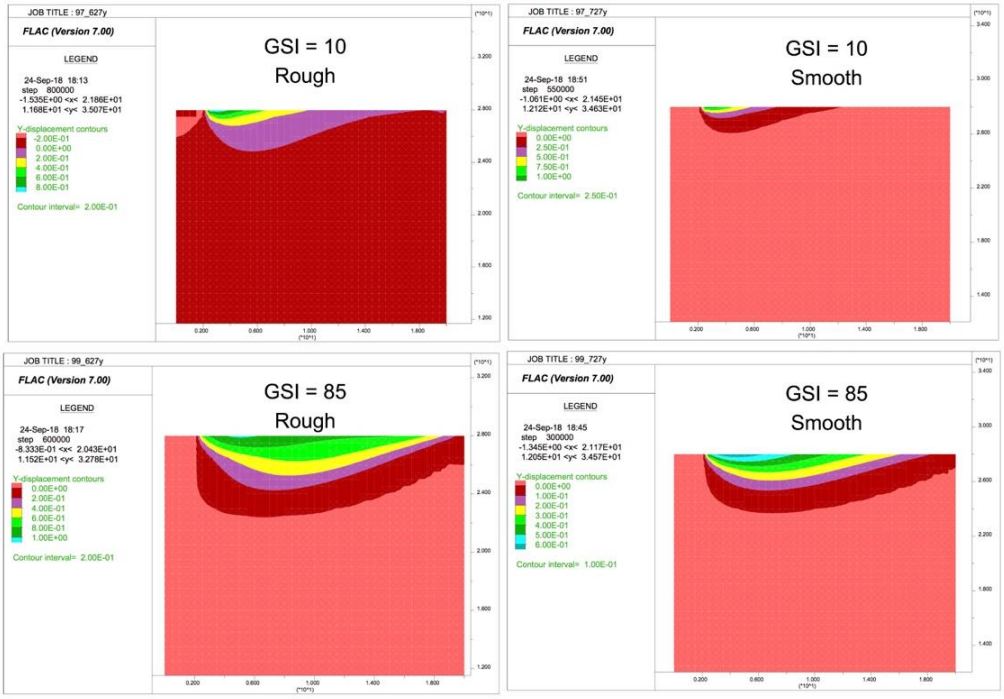

m_o = 20 / B = 4.5 m / UCS = 5 MPa

Fig. 23 The variation of the vertical displacements under the foundation as a function of GSI

Table 7 Summary of the obtained results

P_h (MPa)		Variation between the results (%)		$P_{hSB(estimated)}$ using Eq. (6) (MPa)
P_{hSB}	P_{hRB}	$P_{hRB}/P_{hSB} - 1$	R_F Eq. (6)	
7.22	8.2	13.57	14.23	7.18

close to 4% for low values of the mo = 5 and 11% for high values of m_o = 32.

The maximum value of dispersion depends on the GSI, when all the cases that exceeded 20% matched with a low value for the GSI = 10. In the column of GSI = 10 it can be observed that for high values of UCS, the maximum dispersion was small. Therefore, it can be concluded that the greatest variation between the results of P_{hRB} and P_{hSB} were associated with low values of UCS and GSI.

In Fig. 17(c), the correlation between P_{hRB} and P_{hSB} depending on the UCS, and Fig. 18 an influence of the UCS on the dispersion range was observed in cases of low values of GSI. For average and high GSI values, the relation between P_{hRB} and P_{hSB} was independent from the UCS.

To analyze which was the most conditional parameter in the correlation between P_{hRB} and P_{hSB}, Fig. 19 shows the influence of the m_o as a function of the GSI, and the influence of GSI depending on the mo. This statement can be confirmed from Fig. 19 where GSI was the parameter that most influenced the bearing capacity calculated with different roughness interface. The influence of the GSI was related, as in section 3 for the analysis of the shape factor, to the instantaneous friction angle value: hence with the increase of GSI the influence of the interface type on the ultimate bearing capacity was reduced. It is clear that for GSI close or greater than 50, the range between P_{hRB} and P_{hSB} is less than 20%.

It is also confirmed that the rock type is associated with the dispersion of the results with rough and smooth interface, decreasing the dispersion range with the increase of mo value. It is emphasized that for low value of GSI (GSI=10) the variation between P_{hRB} and P_{hSB} reduces with the increases of m_o, and for average and high GSI the variation between the results increases with the increase of m_o.

4.1 Coefficient R_F

Bearing in mind that the most influential parameters were GSI and m_o, the correlation of the results for each value of the GSI was analyzed according to the rock type (m_o): Fig. 20 deduced from Fig. 19(a). To improve this relationship factor R_F was divided by m_o and three equations were obtained and summarized in Table 6.

Therefore, because the equations in Table 6 have the same structure for different values of GSI, a single equation based on GSI was formulated

$$R_F = e^{\frac{100 - GSI}{28}} \cdot m_o^{\frac{GSI-15}{100}} \quad (6)$$

Fig. 21 shows that the percentage variation calculated by Eq. (6) had a good fit in the 192 cases studied, with a variation between the results that did not exceed 4%, thus emphasizing that most of the results were concentrated in the lower left area of the graph.

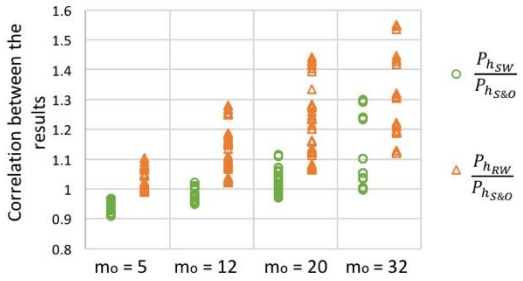

Fig. 24 Correlation between numerical and analytical results of P_h under different foundation base roughness

4.2 Displacement analysis

In this section, we confirm that the horizontal displacement depends on the GSI and the shape of the wedge is the same as observed in soils by Hjiaj (2005). According to Hjiaj in the context of the rough case, a curved rigid wedge immediately underneath the footing can clearly be seen. If the soil-foundation interface is smooth, the soil just below the footing becomes plastic and there is no rigid wedge; these behaviors can be seen in Fig. 22. Furthermore, it is clear that the size of the wedge for smooth footing is smaller than that for an equivalent rough footing (Fig. 22).

Regarding the vertical displacement, it can be observed in Fig. 23 that the behavior and the size of the wedge is similar to the horizontal, thus becoming deeper and bigger with the increase of the GSI value and smaller in cases with smooth interface.

4.3 Example

As an example, we estimated the bearing capacity of the smooth foundation base by calculating the application of the proposed coefficient R_F as defined by eq. (6). We specifically chose the case study in Table 1 with m_o = 12, B = 4.5 m, UCS = 5 MPa and GSI = 50.

The ultimate bearing capacity was calculated numerically by FDM under conditions of smooth (P_{hSB}) and rough (P_{hRB}) interface which were P_{hSB} = 7.22 MPa and P_{hRB} = 8.2 MPa.

The correlation between those two values of the bearing capacity was

$$\frac{P_{h_{RB}}}{P_{h_{SB}}} = \frac{8.2}{7.22} = 1.1357 \qquad \frac{\Delta P_h}{P_{h_{SB}}} = 13.57\%$$

Through the proposed Eq. (6) the difference between the P_{hSB} and P_{hRB} was the following

$$R_F = e^{\frac{100 - GSI}{28}} \cdot m_o^{\frac{GSI-15}{100}} = e^{\frac{100 - 50}{28}} \cdot 12^{\frac{50-15}{100}} = 14.23\%$$

Applying the correction factor R_F, it was estimated that the bearing capacity calculated under the hypothesis of a rough interface was 14% higher than that estimated for the smooth interface. This is important because in cases where the bearing capacity is extremely close to the safety factor,

but it is not enough, a suggestion would be an increase in the rugosity of the base interface to guarantee a greater safety factor.

Therefore, the bearing capacity with smooth interface (P_{hSB}) estimated using factor R_F was

$$P_{h_{SB}} = \frac{P_{h_{RB}}}{1 + \Delta P_h} = \frac{8.2}{1.1423} = 7.18\ MPa$$

Table 7 shows the results obtained from the calculations performed.

It can be concluded that, by the proposed correction factor the bearing capacity of strip foundations on the rock mass under hypothesis of the smooth foundation base was equal to 7.18 MPa. Meanwhile the numerical result was 7.22 MPa, which shows a very effective adjustment, with an error lower than 0.5%.

4.4 Comparison between the results obtained numerically by FDM and analytically by Serrano et al. (2000)

As previously stated, the analytical solution proposed by Serrano *et al.* (2000) cannot include the hypothesis of roughness. However, comparing the results obtained numerically assuming weightless rock mass, associative flow law, plane strain condition and rough interface (P_{hRW}) or smooth interface (P_{hSW}) with the results calculated by the Serrano *et al.* method (2000), Fig. 24 shows that the results are more similar to the values obtained with the smooth interface.

Considering that the analytical formulation does not take into account shear stress on the support level in the stress distribution on the ground, it can be expected that the analytical results to be more similar to the numerical results obtained with a smooth interface.

In addition, it can be observed in Fig. 24 that the dispersion range obtained by comparing P_{hRW} and $P_{hS\&O}$ was higher than that obtained with P_{hSW} and $P_{hS\&O}$, mainly with low and moderate values of mo. Furthermore, the numerical results obtained under the hypothesis of rough interface were always higher than the results of bearing capacity estimated by the analytical method; when applying the smooth interface the numerical results were sometimes lower than the analytical method.

It is important that the results obtained through eq. (6) should not be used directly to increase the bearing capacity estimated by the Serrano *et al.* (2000), for two reasons: (1) the result resemble more the smooth interface, but the method cannot include any hypothesis of roughness; (2) the RF factor was developed considering the self-weight of the material, which is a different hypothesis adopted in the solution proposed by Serrano *et al.* (2000).

5. Conclusions

In our analysis on the influence of the footing shape on the bearing capacity, we took into account the comparison of the numerical results of the bearing capacity of shallow foundations on rock masses, obtained through the FDM under the hypothesis of plane strain, and the axisymmetric conditions, including the associated flow rule, weightless rock mass and rough interface. We can now conclude that:

• The bearing capacity obtained for the circular footing (axisymmetric condition) (P_{hCF}) is at least 35% higher than the bearing capacity for a strip footing (plane strain conditions) (P_{hSF}) of the same width.

• In cases of low values of GSI (e.g., GSI =10) the footing shape shows an important influence on the bearing capacity. This is associated with the fact that the rock mass with low GSI shows a high instantaneous friction angle at the point of failure. It is emphasized that in soil mechanics the friction angle is the parameter that defines the influence of the footing shape on the bearing capacity. The results of the bearing capacity obtained for the circular footing (P_{hCF}) can reach 60% of the results for the strip footing (P_{hSF}).

• The influence of m_o on the bearing capacity with different footing shapes depends on the GSI value. For poor quality rock mass (low value of GSI), the rock type directly affects the correlation between P_{hSF} and P_{hCF}, following the trend that with the increase of mo, the dispersion range of results is reduced.

• The values of the parameters B and the UCS show a negligible influence on the relation between P_{hSF} and P_{hCF}.

• The results of the bearing capacity factor ($N_{\sigma C}$) obtained by the FDM, and applying the proposed factor CF to the analytical formulation of Serrano *et al.* (2000), are very similar to the one proposed by Clausen (2013), with a maximum variation for GSI = 85, ranging from 10% to 17%. There is a great difference between the value of $N_{\sigma C}$ estimated by the formulation proposed by Carter and Kulhawy (1988) and the results obtained by other methods.

• Confirming the theory, that the strip footing can be simulated by several rectangles placed one next to each other, resulting in the overlapping of the bulbs of pressure reaching greater depths, the vertical displacement is deeper in the plane-strain model compared to the axisymmetric model. But when observing the horizontal displacement output it can be concluded that the lateral boundary of the foundation was more affected in the cases of plane strain condition.

Regarding the influence of the roughness interface on the ultimate bearing capacity, from the results obtained with smooth (P_{hSB}) and rough (P_{hRB}) interface, it can be concluded that:

• GSI is the parameter with the most impact on the value of the bearing capacity with different interface roughness. The variation between the results (P_{hSB} and P_{hRB}) decreases with the increase of GSI, and exceeding 20% only in the cases of poor quality rock mass (e.g., GSI = 10).

• With the increase of mo, the dispersion range between P_{hRB} and P_{hSB} decreases, e.g., for m_o = 5 the correlation between the results varies from 3% to 33%, while, for m_o = 32 the range is between 11% to 28%.

• The UCS has little influence on the correlation of the results (P_{hRB}/P_{hSB}), but having more impact on cases with low GSI, while the dispersion range reduces with the increase of the value of UCS.

• Regardless of the calculation method used to obtain the bearing capacity of a strip foundation on rock mass, factor R_F proposed in Eq. (6) can be used to estimate the percentage of variation of the bearing capacity depending

on the roughness of the base interface as function of the geomechanical characteristics (m_o and GSI). According to the analyzed results the value of R_F varies between 3% to 35% depending on the m_o and GSI.

• The correlation of the results of the bearing capacity under hypothesis of the rough and smooth foundation base (P_{hRB} and P_{hSB}) is independent from the footing width.

• The shape of the failure wedge observed numerically by the displacement output of the finite difference method, thus corroborating the results in soils mechanics by Hjiaj (2005).

• The analytical solution proposed by Serrano *et al.* (2000) cannot include any of the hypothesis of the roughness on the foundation base, however, the results of the bearing capacity are very similar to the values obtained numerically with smooth interface, because, the analytical formulation does not include the horizontal stress.

Acknowledgments

The research described in this paper was financially supported by the José Entrecanales Ibarra Foundation.

References

Anil, O., Akbas, S. O., Babagiray, S., Gel, A.C. and Durucan, C. (2017), "Experimental and finite element analyses of footings of varying shapes on sand", *Geomech. Eng.*, **12**(2), 223-238. https://doi.org/10.12989/gae.2017.12.2.223.

Barton, N. (1973), "Review of a new shear-strength criterion for rock joints", *Eng. Geol.*, **7**(4), 287-332. https://doi.org/10.1016/0013-7952(73)90013-6.

Barton, N. and Choubey, V. (1977), "The shear strength of rock joints in theory and practice", *Rock Mech.*, **10**(1-2), 1-65. https://doi.org/10.1007/BF01261801.

Benmebarek, S., Saifi, I. and Benmebarek, N. (2017), "Depth factors for undrained bearing capacity of circular footing by numerical approach", *J. Rock Mech. Geotech. Eng.*, **9**(4), 761-766. https://doi.org/10.1016/j.jrmge.2017.01.003.

Brinch Hansen, J.A. (1970), "Revised and extended formula for bearing capacity" *Bulletin No. 28*. Danish Geotechnical Institute Copenhagen, Denmark, 5-11.

Carter, J.P. and Kulhawy, F.H. (1988), "Analysis and design of foundations socketed into rock", Report No. EL-5918, Empire State Electric Engineering Research Corporation and Electric Power Research Institute, New York, U.S.A., 158.

Chakraborty, M. and Kumar, J. (2015), "Bearing capacity of circular footings over rock mass by using axisymmetric quasi lower bound finite element limit analysis", *Comput. Geotech.*, **70**, 138-149. https://doi.org/10.1016/j.compgeo.2015.07.015.

Clausen, J. (2013), "Bearing capacity of circular footings on a Hoek–Brown material", *Int. J. Rock Mech. Min. Sci.*, **57**, 34-41. https://doi.org/ 10.1016/j.ijrmms.2012.08.004.

De Beer, E.E. (1970), "Experimental determination of the shape factors and the bearing capacity factors of sand", *Géotechnique*, **20**(4), 387-411. https://doi.org/10.1680/geot.1970.20.4.387.

Du, S., Gao, H., Hu, Y., Huang, M. and Zhao, H. (2015), "A new method for determination of joint roughness coefficient of rock joints", *Math. Prob. Eng.*, 1-6. https://doi.org/10.1155/2015/634573.

FLAC (2007), *User's Manual*, Itasca Consulting Group Inc., Minneapolis, Minnesota, U.S.A.

Ghosh, A.K. (2010), "Shear strength of dam-foundations rock interface—a case study", *Proceedings of the Indian Geothecnical Conference*, Mumbai, India, December.

Gutiérrez-Ch, J.G., Senent, S., Melentijevic, S. and Jimenez, R. (2018), "Distinct element method simulations of rock-concrete interfaces under different boundary conditions", *Eng. Geol.*, **240**, 123-139. https://doi.org/10.1016/j.enggeo.2018.04.017.

Hjiaj, M., Lyamin, A.V. and Sloan, S.W. (2005), "Numerical limit analysis solutions for the bearing capacity factor Nγ", *Int. J. Solids Struct.*, **42**(5-6), 1681-1704. https://doi.org/10.1016/j.ijsolstr.2004.08.002.

Hoek, E. and Brown, E.T. (1980), "Empirical strength criterion for rock masses", *J. Geotech. Eng. Div.*, **106**(9), 1013-1035.

Hoek, E. and Brown, E.T. (1997), "Practical estimates of rock mass strength", *Int. J. Rock Mech. Min. Sci.*, **34**(8), 1165-1186. https://doi.org/10.1016/S1365-1609(97)80069-X.

Jahanandish M., Veiskarami, M. and Ghahramani, A. (2012), "Effect of foundation size and roughness on the bearing capacity factor, N γ , by stress level-based ZEL method", *Arab. J. Sci. Eng.*, **37**(7), 1817-1831. https://doi.org/10.1007/s13369-012-0293-3.

Jeong, S., Ahn, S. and Seol, H. (2010), "Shear load transfer characteristics of drilled shafts socketed in rocks", *Rock Mech. Rock Eng.*, **43**(1), 41-54. https://doi.org/10.1007/s00603-009-0026-4

Keshavarz, A. and Kumar, J. (2018), "Bearing capacity of foundations on rock mass using the method of characteristics", *Int. J. Numer. Anal. Meth. Geomech.*, **42**(3), 542-557. https://doi.org/10.1002/nag.2754.

Krounis, A., Johansson, F. and Larsson, S. (2016), "Shear strength of partially bonded concrete–rock interfaces for application in dam stability analyses", *Rock Mech. Rock Eng.*, **49**(7), 2711-2722. https://doi.org/10.1007/s00603-016-0962-8.

Lo, K.Y., Lukajic, B., Wang, S., Ogawa, T. and Tsui, K.K. (1990), "Evaluation of strength parameters of concrete-rock interface for dam safety assessment", *Proceedings of the Canadian Dam Safety Conference*, Toronto, Canada, September.

Lo, K.Y., Ogawa, T., Lukajic, B. and Dupak, D.D. (1991), "Measurement of strength parameters of concrete-rock contact at the dam foundation interface", *Geotech. Test. J.*, **14**(4), 383-394. https://doi.org/10.1520/GTJ10206J.

Maleki, H. and Hollberg, K., (1995), "Structural stability assessment through measurements", *Proceedings of the ISRM International Workshop on Rock Foundations*, Tokyo, Japan, September.

Melentijevic, S. and Olalla, C. (2014), "Different FEM models for simulation of the Osterberg load test in rock shafts", *Proceedings of the ISRM Regional Symposium EUROCK 2014*, Vigo, Spain, May.

Merifield, R.S., Lyamin, A.V. and Sloan, S.W. (2006), "Limit analysis solutions for the bearing capacity of rock masses using the generalised Hoek–Brown criterion", *Int. J. Rock Mech. Min. Sci.*, **43**(6), 920-937. https://doi.org/10.1016/j.ijrmms.2006.02.001.

Meyerhof, G.G. (1955), "Influence of roughness of base and ground-water conditions on the ultimate bearing capacity of foundations", *Geotechnique*, **5**(3), 227-242. https://doi.org/10.1680/geot.1955.5.3.227.

Meyerhof, G.G. (1963), "Some recent research on the bearing capacity of foundations", *Can. Geotech. J.*, **1**(1), 16-26. https://doi.org/10.1139/t63-003.

Mouzannar, H., Bost, M., Leroux, M. and Virely, D. (2017), "Experimental study of the shear strength of bonded concrete–rock interfaces: Surface morphology and scale effect", *Rock Mech. Rock Eng.*, **50**(10), 2601-2625. https://doi.org/10.1007/s00603-017-1259-2.

Nam, M.S. and Vipulanandan, C. (2008), "Roughness and unit

side resistances of drilled shafts socketed in clay shale and limestone", *J. Geotech. Geoenviron. Eng.*, **134**(9), 1272-1279. https://doi.org/10.1061/(ASCE)1090-0241(2008)134:9(1272).

Nitta, A., Yamamoto, S., Sonoda, T. and Husono, T. (1995), "Bearing capacity of soft rock foundation on in-situ bearing capacity tests under inclined load." *Proceedings of the ISRM International Workshop on Rock Foundations*, Tokyo, Japan, September.

Pellegrino, A. (1974), "Surface footings on soft rocks", *Proceedings of the 3rd Congress of the International Society for Rock Mechanics*, Denver, Colorado, U.S.A., September.

Pells, P.J.N. and Turner, R.M. (1979), "Elastic solutions for the design and analysis of rocksocketed piles", *Can. Geotech. J.*, **16**(3), 481-487. https://doi.org/10.1139/t79-054.

Pells, P.J.N., Rowe, R.K. and Turner, R.M. (1980), "An experimental investigation into side shear for socketed piles in sandstone", *Proceedings of the International Conference on Structural Foundations on Rock*, Sydney, Australia, May.

Ramamurthy, T. (2014), *Engineering in Rocks for Slopes Foundations and Tunnels*, PHI Learning, Delhi, India.

Rowe, R.K. and Armitage, H.H. (1984), "The design of piles socketed into weak rock", Report GEOT-11-84, University of Western Ontario, London, Canada.

Samanta, M., Punetha, P. and Sharma, M. (2018), "Effect of roughness on interface shear behavior of sand with steel and concrete surface", *Geomech. Eng.*, **14**(4), 387-398. https://doi.org/10.12989/gae.2018.14.4.387.

Seidel, J.P. and Collingwood, B. (2001), "A new socket roughness factor for prediction of rock socket shaft resistance", *Can. Geotech. J.*, **38**(1), 138-153. https://doi.org/ 10.1139/t00-083.

Serrano, A., Olalla, C. and González, J. (2000), "Ultimate bearing capacity of rock masses based on the modified Hoek-Brown criterion", *Int. J. Rock Mech. Min. Sci.*, **37**(6), 1013-1018. https://doi.org/ 10.1016/S1365-1609(00)00028-9.

Sokolovskii, V.V. (1965), *Statics of Soil Media*, Butterworths Science, London, U.K.

Spanovich, M. and Garvin, R.G. (1979), *Field Evaluation of Caisson-Shale Interaction*, in *Behavior of Deer, Foundations (STP 670)*, ASTM, 537-557.

Tajeri, S., Sadrossadat, E. and Bazaz, J.B. (2015), "Indirect estimation of the ultimate bearing capacity of shallow foundations resting on rock masses", *Int. J. Rock Mech. Min. Sci.*, **80**, 107-117, https://doi.org/10.1016/j.ijrmms.2015.09.015.

Terzaghi, K. (1943), *Theoretical Soil Mechanics*, Wiley, New York, U.S.A.

Tikou, B. (2016), "Quantitative parameters of primary roughness for describing the morphology of surface discontinuities at various scales", *Geomech. Eng.*, **11**(4), 515-530. https://doi.org/10.12989/gae.2016.11.4.515.

Tse, R. and Cruden, D.M. (1979), "Estimating joint roughness coefficients", *Int. J. Rock Mech. Min. Sci. Geomech. Abstr.*, **16**(5), 303-307. https://doi.org/10.1016/0148-9062(79)90241-9.

Vesic, A.S. (1973), "Analysis of ultimate loads of shallow foundations", *J. Soil Mech. Found. Div.*, **99**, 45-73.

Williams, A.F. (1980), "Design and performance of piles socketed into weak rock", Ph.D. Dissertation, Monash University, Melbourne, Australia.